Operando and ex-situ investigation of PEMFC degradation

P. Gazdzicki[a], J. Mitzel[a], D. G. Sanchez[a], P. Aßmann[a], J. Sousa[a], T. Morawietz[a,b,c], R. Hiesgen[b†], F. Häußler[d], J. Hunger[d], G. Schlumberger[d] , K. A. Friedrich[a,c]

[a] German Aerospace Center (DLR), 70569 Stuttgart, Germany
[b] University of Applied Sciences Esslingen, 73728 Esslingen, Germany
[c] University of Stuttgart, 70569 Stuttgart, Germany
[d] Zentrum für Sonnenenergie- und Wasserstoff-Forschung, 89081 Ulm, Germany
[†]deceased

Longevity is one of key requirements of PEMFCs for automotive applications. Hence, understanding degradation phenomena and durability limitations is fundamental to increase PEMFC life time and to make this technology competitive. In this contribution a selection of our recent work on these topics is presented. In particular, attention is dedicated to study effect of performance limitations at low Pt loadings and to investigate impact of operation conditions on local degradation phenomena such as drying, contaminations or heterogeneities during dynamic operation. Moreover, specific operando accelerated stress tests are being developed and the relative impact on various stressors on individual MEA components is studied. Eventually, we present results related to on-line fault monitoring using current density distribution measurements linked with impedance spectroscopy.

Introduction

To be competitive to internal combustion engines (ICE), polymer electrolyte membrane fuel cells (PEMFC) have to achieve a targeted lifetime of 5000 - 6000 h in case of passenger cars. For heavy duty applications the required lifetime is even higher with targeted values of 20,000 h. This includes dynamic PEMFC operation as well as various critical events such as shut-down and start-up or operation under extreme conditions (freezing or hot). All of these conditions have impact on changes of components of the membrane electrode assembly (MEAs) over time due to numerous chemical and physical degradation effects. Even though significant progress has been made towards understanding of PEMFC degradation, the required lifetime is still >20% below the 2020 target for automotive application defined by the European Commission [1] or the US Department of Energy [2].

During PEMFC durability tests numerous processes are involved that lead to performance losses which make the interpretation of such tests difficult [3]. Hence, to discriminate between different phenomena, it is necessary to study degradation in certain relevant conditions and using specific stressors separately.

Moreover, PEMFCs with low Pt loadings are demonstrating continuous progress in terms of performance and durability. Thereby, the reduction of Pt content in FCEVs is not primarily motivated by reducing cost, but rather to avoid increasing the Pt demand

due to future mass production of fuel cell electric vehicles (FCEVs). Therefore, the total amount of Pt used in FCEV should not exceed the Pt content required for catalytic exhaust converters of ICE cars equaling approximately 6 g Pt per car [3]. Consequently, the Pt loading of MEAs should be as low as 0.1 mg cm^{-2} assuming a car with 90-100 kW average power [4] and a peak power of the PEMFC of 1 W cm^{-2} [1]. This means a drastic reduction of current state-of-the-art Pt loading (~0.3-0.4 mg cm^{-2}) which leads to severe performance and durability limitations that need to be mitigated. Currently, local oxygen transport resistance of the cathode [6] is considered as the main hurdle limiting performance at high current density. In contrast, the reduction of anodic Pt loading down to 0.05 mg cm^{-2} does not influence cell performance [7].

In this paper we present an overview of various activities linked to understanding of PEMFC degradation at the single cell and stack level. At single cell level we link operation conditions and stressors with local degradation effects by monitoring local current density distribution. Furthermore, we study the impact of various stressors such as freezing, mechanical stress or excess temperature. At stack level we present results on the impact of Pt loading on performance degradation as well as how to monitor state-of-health during operation by linking local current density distribution with electrochemical impedance spectroscopy (EIS).

Experimental

Single cell tests were performed using gold coated stainless steel cells with 25 cm^2 active area and single serpentine flow field or 142 cm^2 active area and multi-serpentine flow field designed at DLR. Moreover, a Baltic Fuel Cells single cell with 25 cm^2 and multi-serpentine flow field was used as well. The stack tests to study impact of Pt loading on performance losses have been conducted using DLR home-made research stack with graphitic bipolar plates of 142 cm^2 active area (see Figure 1 (A)) described in [8] in detail. The cells were typically operated using Harmonized European Test Protocols [9]. To study on-line fault diagnostics a liquid-cooled PEMFC stack manufactured by ZSW (Zentrum für Sonnenenergie- und Wasserstoff-Forschung Baden-Württemberg) was used. This stationary stack of 480 W nominal electrical power output was equipped with ten single cells of 96 cm^2 active electrode area using graphitic composite bipolar plates. Three printed circuit boards (PCBs) for measuring the current density distribution were included in the stack. The first PCB was integrated at cell 01 close to the anodic current collector, the second PCB in the middle of the stack (between cell 05 and cell 06) and the third PCB at cell 10 close to the cathodic current collector and the media supply ports as shown in Figure 1 (B).

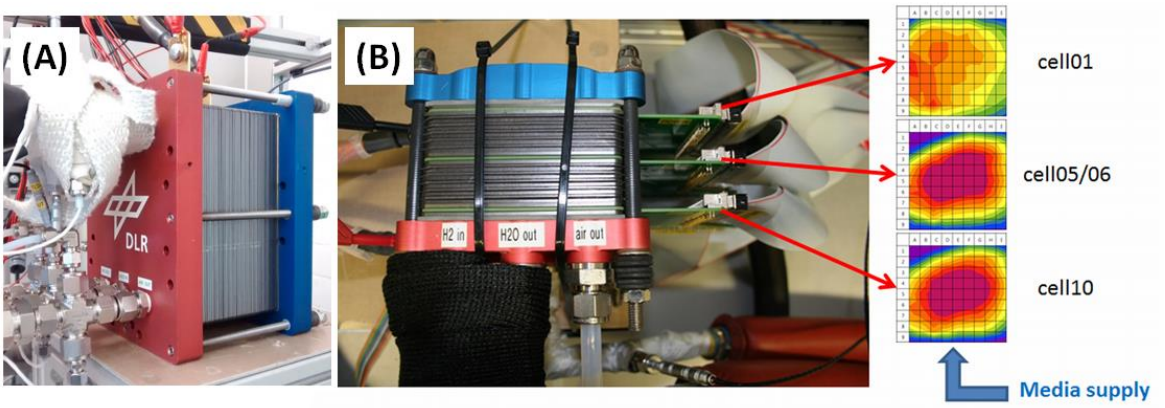

Figure 1: (A): Stack to study impact of Pt loading on performance decay. (B) Setup for on-line fault diagnostics and state-of-health monitoring.

The tests have been performed using DLR's in-house developed test stands controlled by programmable logic controllers that allow automatic control of the input and output conditions, such as the pressure, temperature, gas flow rates and humidity. The DLR patented technology of segmented bipolar plates based on PCBs is used for current density distribution measurements. The used PCBs were specially designed for the different used test setups and were manufactured by Axel Helmbold Messtechnik. The data acquisition was realized using Multifunction Switch/Measure Units (Keysight Technologies) and data processing and visualization was carried out using an in-house programmed LabView application.

For EIS data acquisition and analysis a combined device for parallel single cell measurements by ZAHNER-elektrik GmbH & Co. KG was used. Measurements were realized in galvanostatic EIS mode. An electronic load EL1000 was used to apply the sinoidal current signal to the entire stack. An IM6 potentiostat equipped with three PAD4 modules was used to measure the voltage responses of the 10 single cells. Data acquisition and analysis was carried out using the Thales XT 5.2.0 software.

In each section is indicated which kind of test hardware was used. The MEAs used in these studies were different commercial products with Pt/C catalysts obtained from EWII Fuel Cells, Johnson Matthey, Greenerity or Ion Power.

Results and Discussion

Impact of Pt loading on performance decay

To study the influence of Pt loading on performance and degradation a DLR-developed 19 cells rainbow stack (equipped with MEAs of different Pt loading) with 142 cm^2 active area was operated in continuous dynamic operation using the fuel cell dynamic load cycle (FC-DLC) with hydrogen and air supplied in a counter-flow configuration. For details on the test protocol the reader is referred to [8]. Stack operating parameters have been controlled following the testing procedures developed in the European Stack-Test project [10,11].

Figure 2 (A) and (B) shows the evaluation of beginning-of-test (BoT) single cell voltages at different anodic and cathodic Pt loadings. Apparently and in agreement with

literature [7] anodic loading does not affect BoT performance in the studied range. In case of cathodic Pt loading, however, a strong dependence is observed on the cell voltage. According to the data in panel (B) a cathodic Pt loading of around 0.2 mg cm^{-2} is found to be a threshold value; below this value the cell performance drops significantly for current densities >1 A cm^{-2} which is likely associated with high oxygen mass conversion rates in the thin catalyst layers (note: Pt loading in the MEAs was adjusted by varying the layer thickness at a constant Pt/C ratio).

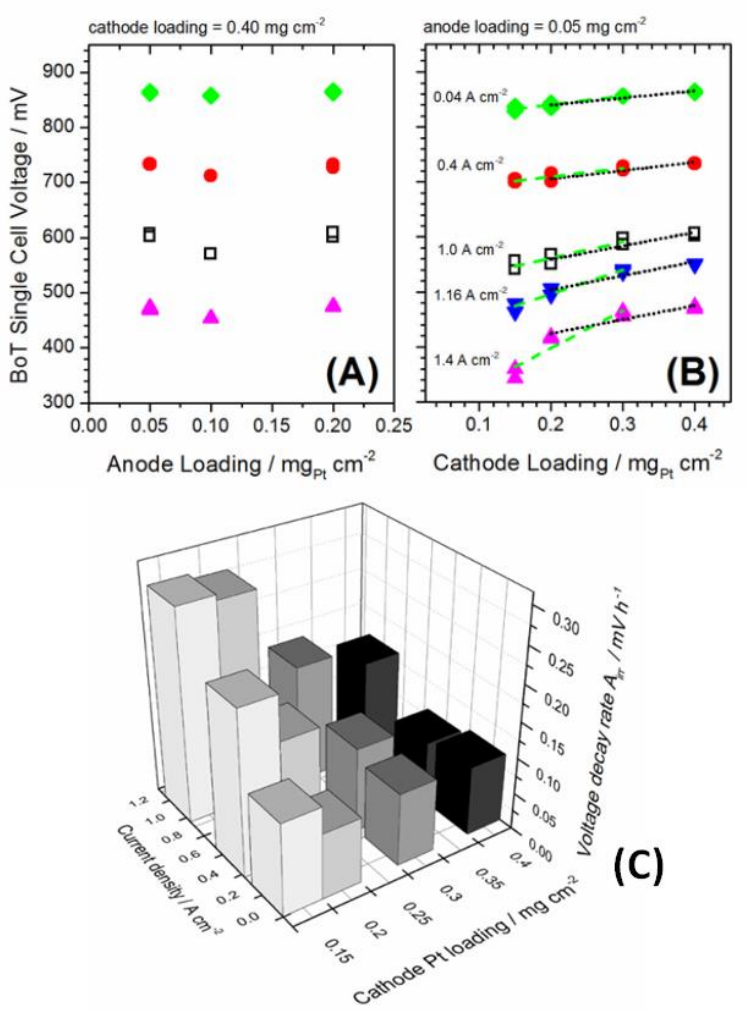

Figure 2: Effect of Pt loading on performance and irreversible degradation. (A) Single cell BoT voltages versus anode Pt loading. (B) Single cell BoT voltages versus cathode Pt loading. The different data points correspond to different current densities as indicated in the figure. The dashed and dotted lines are linear regressions of data in the cathodic Pt loading ranges 0.20 – 0.40 mg cm^{-2} (high Pt loadings) and 0.05 – 0.30 mg cm^{-2} (low Pt loadings), respectively. (C) Irreversible voltage decay rate as a function of current density and cathode Pt loading determined from a rainbow stack equipped with MEAs of different Pt loading. Reprinted from Fuel Cells, Vol. 18, Gazdzicki, P., Mitzel, J., Dreizler, A.M., Schulze, M., Friedrich, K.A., Impact of Platinum Loading on Performance and Degradation of Polymer Electrolyte Fuel Cell Electrodes Studied in a Rainbow Stack, Pages 270-278, Copyright (2018), with permission from Wiley.

Apart from BoT performance limitations at low Pt loadings it is necessary to evaluate the impact of Pt loading on long-term operations. For this purpose, Figure 2 (C) presents the irreversible degradation as a function of current density and cathodic Pt loading (anodic Pt loading had no measurable influence on irreversible degradation). The irreversible degradation rates are determined from continuous FC-DLC load cycling tests of ~ 500 h [8] which represent accelerated stress testing [3]. At low current densities a largely constant irreversible degradation rate is observed: at higher current densities, on the other hand, the irreversible degradation rate increases dramatically for cathodic Pt loadings $\leq$ 0.2 mg cm^{-2}. Accordingly, a cathodic Pt loading 0.2–0.3 mg cm^{-2} represents a threshold value below which the cathode leads to a significantly increased irreversible degradation.

This effect could be caused by a faster increasing mass transport resistance at low Pt loadings [12]. This result clearly demonstrates that when going to ultra-low Pt loadings such as 0.1 mg cm^{-2} requires deep understanding of transport limitations occurring in the cathode catalyst layer in order to propose improvements to mitigate these limitations not only at BoT but also upon long term operation.

Linking degradation with local operation conditions

Constant versus dynamic operation. Fuel cell operation may lead to heterogeneous operation conditions due to drying, flooding or impurities. Therefore, operando electrochemical investigations including monitoring of local operation conditions have been carried out in a broad range of operation conditions to i) study the impact of operation conditions on degradation and ii) identify impact of impurities on local degradation. The MEAs used in this study consisted of a commercial catalyst coated membrane (MEA0476) from Johnson Matthey Fuel Cells and Sigracet 25 BC gas diffusion layers (GDLs) from SGL Carbon GmbH.

Figure 3 depicts irreversible degradation of five single cell (DLR cell with 25 cm^2 active area) durability tests. These tests include load cycling in different current density ranges. The load cycles are (i) low potential cycling (10 s at OCV/ 10s at 0.2 A cm^{-2}) and (ii) high potential cycling (10 s at OCV or 0.2 A cm^{-2} / 10 s at 1 A cm^{-2}) with ~500 h. Moreover, two tests at constant load of 0.1 A cm^{-2} and 1 A cm^{-2} have been performed for comparison. The degradation rates have been determined from polarization curves at BoT, EoT and from characterizations in-between. All tests have been carried out using a segmented cell for operando monitoring of current density distribution [13].

Generally, the results demonstrate that dynamic load cycling leads to lower voltage losses compared to operation at constant current independent on the applied current density. In other words, constant operation at 0.1 A cm^{-2} and 1 A cm^{-2} yields highest degradation rate linked with a significant increase of the ohmic and mass transport resistance (not shown). The degradation at high voltage is usually addressed to carbon corrosion leading to catalyst layer degradation with negative effect on water management [14] and to radical formation and attack of the ionomer leading to reduced ionic conductivity [15].

Moreover, the high voltage losses at constant current operation are related to strongly heterogeneous current density distributions as shown in the top right inset of Figure 3 for the constant load test performed at 0.1 A cm^{-2}. It is noted, that a similar heterogeneous current density distribution was observed for the constant load test performed at 1.0 A cm^{-2} as well. In contrast, dynamic tests with relatively low voltage losses show a much more homogenous current density distribution (bottom right inset). During load cycling the detrimental conditions that lead to heterogeneities in current density occur only during short periods of time and are continuously recovered due to dynamic operation; however, in case of constant load operation recovery procedure is absent and the heterogeneities are reinforced with time.

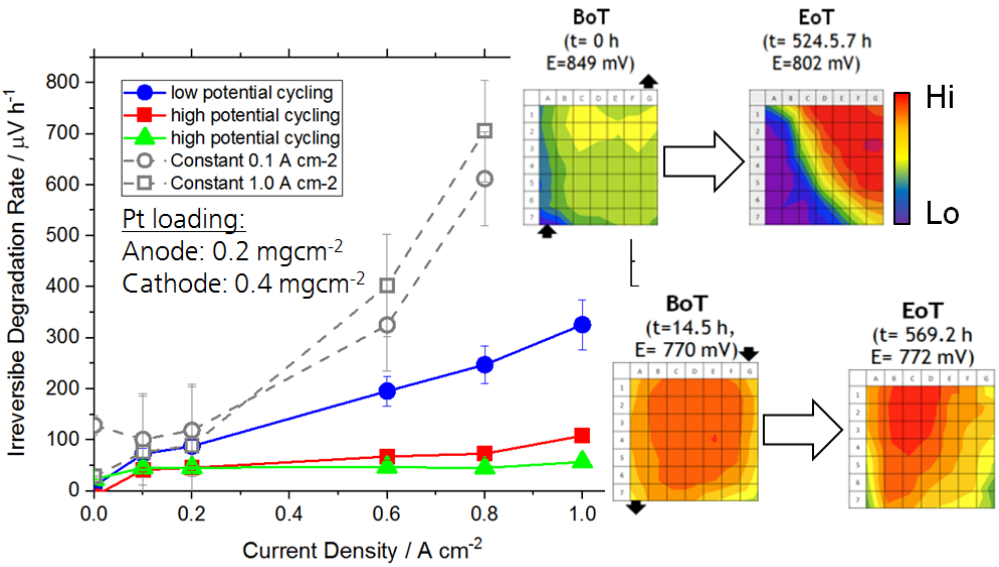

Figure 3: Irreversible degradation of ~ 500 h tests performed at different operation conditions (cycling and constant load as indicated in the figure) along with current density distributions recorded at BoT and EoT in a constant load at 0.1 A cm^{-2} and a dynamic cycling test.

After the durability test the structural degradation of the cycled cells was evaluated by scanning electron microscopy (SEM) analysis of MEA samples from selected segments. A typical freeze-fractured MEA depicted in Figure 4 (A) shows a sample from a load cycling test as an example. The sample was cut from a segment which exhibited particularly high current density during operation as indicated in the figure. Apparently the MEA exhibits Pt particles in the membrane (proven by EDX). The bar chart in Figure 4 (B) shows the amount of Pt particles in the membrane measured with SEM in areas of 15 x 15 µm² in front of the cathode. The highest Pt concentrations are observed after load cycling at high voltages and in segments with high current density. The Pt band in the membrane develops due to Pt dissolution in the cathode [16,17], ion migration across the membrane and subsequent Pt reduction by hydrogen that permeates from the anode side. Thereby, the position of Pt deposition is determined by the partial pressures of hydrogen and oxygen [18].

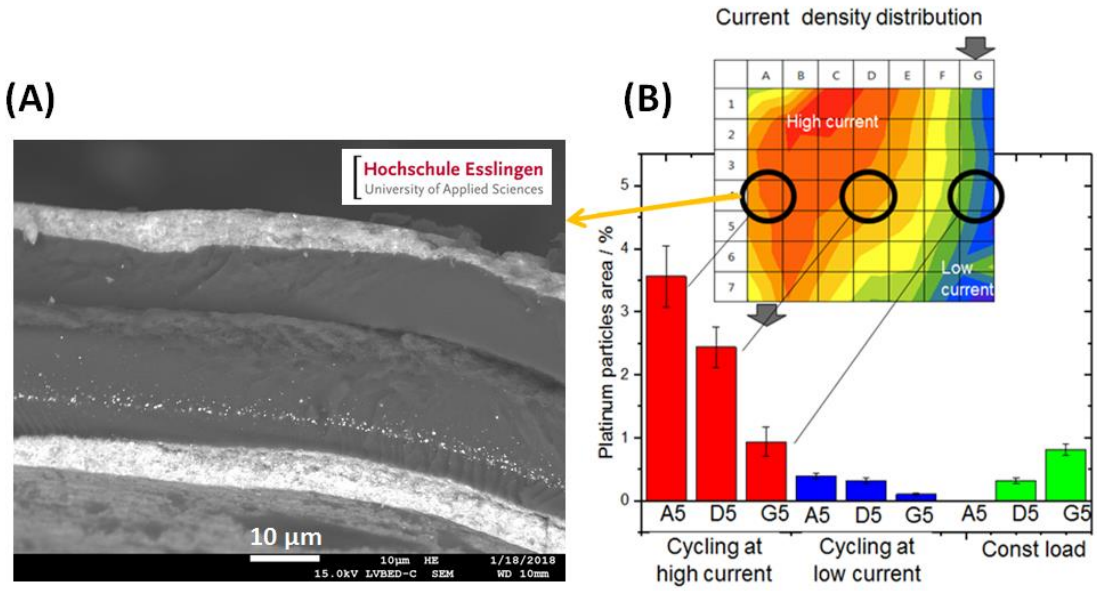

Figure 4: Link between local operation conditions and local degradation. (A) SEM image of a MEA segment showing particularly high current density after ~500 h load cycling. (B) Local current density distribution along with amount of Pt particles in the membrane (Pt band) determined by SEM in the indicated segments for two load cycling and one constant load durability test.

Local effect of impurities. In addition of studying degradation effects caused by operation conditions, we also provide an analysis of effects of different externally introduced contaminants. These include silicon from gasket and nickel from defective gold coatings of the flow field. The study was carried out in 142 cm^2 single cell using segmented cell to measure current density distribution; the corresponding durability tests were performed in fully humidified and non-humidified conditions [19]. The MEAs used in this study were commercial Nafion® XL membrane coated with a Pt/C based catalyst layer with Pt loading of 0.3 $mgcm^{-2}$ on both sides placed between Sigracet 25 BCE gas GDLs from SGL Carbon. The test in non-humidified conditions is shown in Figure 5. Apparently, the voltage drop is linked with a significant change of current density distribution which leads to performance loss especially in the air inlet area (column H and I). The segments labelled by the circles were analyzed by EDX after EoT. The results shown in Figure 6 indicate traces of Ni and Si in the membrane and the electrodes, as well as Pt in the membrane. It is noted that the uncertainty of the amount of these trace elements is high and the analysis can only be considered as qualitative. It indicates Pt in the membrane close to air outlet (column C) as well in areas which exhibited particularly high current density during operation (Column D); the latter observation is in agreement with the results shown in Figure 4 in the previous subsection. Moreover, Ni contamination was detected primarily close to edge areas of the MEA which explains the strong irreversible degradation of cell performance in these areas. On the other hand, degradation induced by Si contamination is found to be at least partially reversible and can be prevented by presence of liquid water; accordingly, degradation in areas of water accumulation (bottom of the cell due to influence of gravity) can be linked to Ni contamination as confirmed by the post mortem analysis [19].

Compared with Si contamination or membrane dehydration, performance losses due to Ni contamination occur more slowly. However, Ni contaminations generate irreversible degradation which is particularly detrimental.

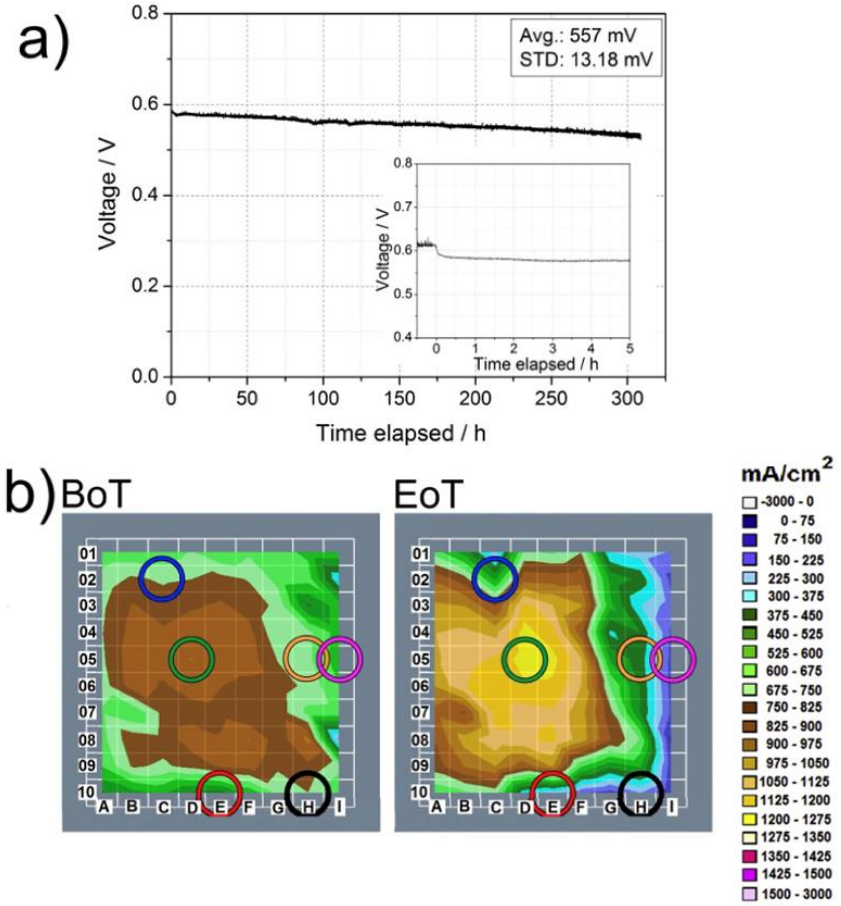

Figure 5: Cell operation under non-humidified gas supply (approx. 5% RH). A) Development of cell voltage during 300 h operation at 0.7 A cm^{-2} and 60 °C cell temperature. The inset shows the voltage decay in the first 5 h. At 0 h, the gas humidification was switched off. B) Current density distributions at BoT and EoT. The colored circles indicate the segments that were investigated by ex-situ methods after EoT. (see Figure 6). Cathode inlet/anode outlet and cathode outlet/anode inlet areas are located at row I and A, respectively. Reprinted from Journal of Power Sources, Vol 352, Daniel G. Sanchez, Tiziana Ruiu, Indro Biswas, Mathias Schulze, Stefan Helmly, K. Andreas Friedrich, Local impact of humidification on degradation in polymer electrolyte fuel cells, Pages 42-55, Copyright 2017, with permission from Elsevier.

Segment	Ni/wt%					Si/wt%					Pt/wt%	
	An-M	PTFE	Ca-M	An	Ca	An-M	PTFE	Ca-M	An	Ca	PTFE	Ca-M
C2	3.4 ± 2.9	2.6 ± 2.3	3.6 ± 3.2	–	0.5 ± 0.9	2.3 ± 0.7	0.3 ± 0.1	1.5 ± 0.7	1.1 ± 0.5	–	0.4 ± 0.4	0.2 ± 0.2
D5	0.1 ± 0.1	<0.1	0.2 ± 0.2	–	–	2.2 ± 0.5	0.3 ± 0.3	1.4 ± 0.6	–	0.3 ± 0.5	0.7 ± 0.6	0.1 ± 0.1
H5	–	–	–	–	–	0.6 ± 0.2	0.1 ± 0.1	0.7 ± 0.2	–	0.5 ± 0.2	<0.1	0.3 ± 0.1
I5	–	0.2 ± 0.2	<0.1	–	–	3.2 ± 0.6	<0.1	2.3 ± 0.5	1.4 ± 0.8	1.2 ± 0.6	–	0.2 ± 0.4
E10	2.9 ± 0.4	1.8 ± 0.9	2.8 ± 0.3	0.5 ± 0.2	0.2 ± 0.2	2.7 ± 0.6	0.2 ± 0.1	2.6 ± 0.0	0.8 ± 0.4	1.9 ± 0.3	–	0.2 ± 0.3
H10	–	–	–	–	–	2.4 ± 0.5	0.3 ± 0.3	1.9 ± 0.2	1.2 ± 1.1	2.4 ± 1.3	0.1 ± 0.2	–
Pristine MEA	–	–	–	–	–	2.0 ± 0.7	0.1 ± 0.1	1.5 ± 0.6	–	–	–	–

Figure 6: Result of the quantitatively analyzed EDX spectra of samples stemming from the indicated areas of the MEA. Given values are averaged from at least three measured values. An-M and Ca-M indicate analysis results of membrane samples at the anode and cathode side, respectively; PTFE indicates the membrane PTFE reinforcement layer; An and Ca refer to analysis of anode and cathode catalyst layer, respectively. Reprinted from Journal of Power Sources, Vol 352, Daniel G. Sanchez, Tiziana Ruiu, Indro Biswas, Mathias Schulze, Stefan Helmly, K. Andreas Friedrich, Local impact of humidification on degradation in polymer electrolyte fuel cells, Pages 42-55, Copyright 2017, with permission from Elsevier.

Accelerated Stress Tests

Specific in-situ ASTs. In order to understand the impact of specific stressors on individual MEA components in-situ ASTs were studied focusing on mechanical stress cycling, excess temperature operation and freeze-thaw cycling (see next subsection). These tests were carried out using 25 cm^2 Baltic Fuel Cells test hardware. The used catalyst coated membranes were from Johnson Matthey Fuel Cells which were placed between commercial carbon fiber based GDLs.

Although in-situ ASTs exist for the membrane and the catalyst layer, no in-situ ASTs are available for the GDL so far. Hence our current activity is focused on the development of GDL specific ASTs and quantification of their impact on degradation of individual MEA components.

In Figure 7 (A) and (B) performance curves obtained during two different ASTs are compared:

- In panel (A) data of the mechanical stress test is shown: the cell was operated at 1 A cm^{-2} at 80°C, stoichiometry of 1.5 for H_2 and air. To induce stress the cell temperature was continuously cycled between 60°C and 95°C while keeping the absolute water contend in the feed gases constant leading to cycling of the RH between 120% and 30%. The test was composed of around 150 cycles.

- In panel (B) data of excess temperature AST is shown: the cell was operated for 245 h at 1 A cm^{-2} at increased cell temperature of 95°C, 50% RH and stoichiometry of 1.5 for H_2 and air.

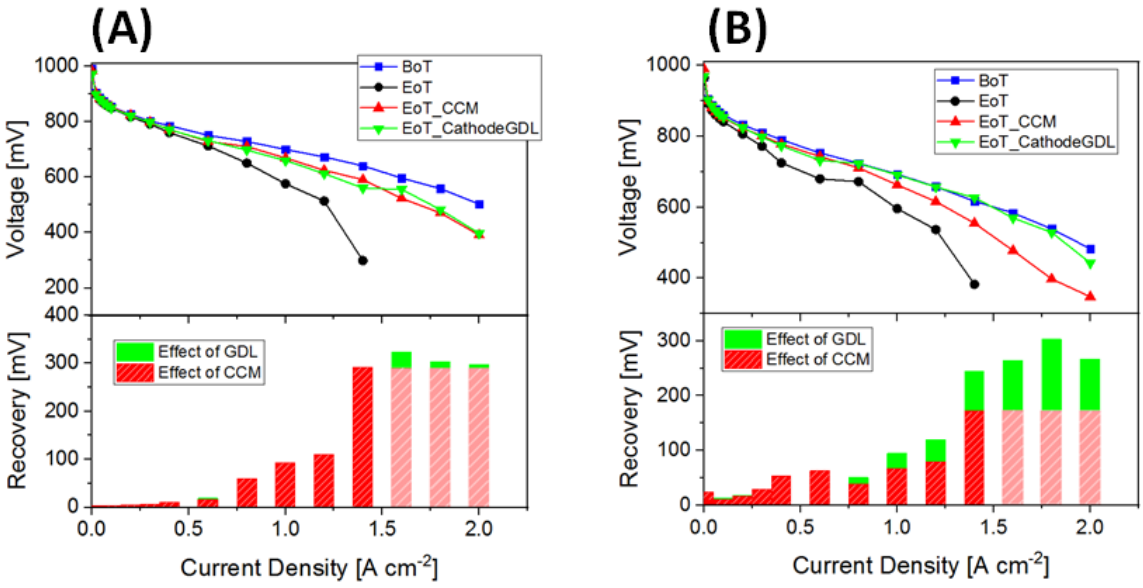

Figure 7: Performance evaluation during in-situ ASTs recorded at EoT, BoT, after exchanging the aged CCM by a new one (BoT_CCM) and after subsequently exchanging the aged cathode GDL by a new one (EoT_Cathode). (A) Performance curves and voltage recovery due to effect of CCM and GDL for a "mechanical stress AST". (B) Performance curves and voltage recovery due to effect of CCM and GDL in case of "excess temperature AST". The CCM contribution to recovery at >1.5 A cm^{-2} cannot be calculated due to lack of data of the EoT performance curve. The bright patterned boxes were therefore assumed as lower limits for the CCM effects.

In both cases after EoT characterization the aged CCM was replaced by a new one and the cell was characterized (EoT_CCM) again. Eventually, the aged cathode GDL was replaced by a new GDL followed by a final EoT_CathodeGDL characterization to distinguish between the impact of the CCM and the GDL on the observed performance losses. The bottom panels show the voltage recovery due to replacing the CCM and the GDL separately. It is evident, that in case of the mechanical stress test, replacing the CCM leads to substantial voltage recovery; subsequently replacing the GDL does not lead to any significant improvement. Consequently, mechanical stress leads to mainly CCM degradation. Most likely, degradation of the cathode catalyst layer is the key issue leading to severe increase of charge transfer and mass transport resistance (EIS not shown). Degradation of membrane cannot be ruled out, but there is no direct indication based on changes of the ohmic resistance. On the other hand, the excess temperature test leads to less CCM degradation than the mechanical cycling test. However, there is strong indication of GDL degradation especially relevant at current densities >1.2 A cm^{-2}. It is noted that this effect may have some contribution due to disassembly and reassembly of the cell for exchanging the aged components. According to EIS measurements replacing the aged CCM leads to a reduction of the cell impedance by 0.7 mOhm cm^2 while replacing the aged GDL leads to an additional reduction by ~0.2 mOhm cm^2. This shows that also in this case the cathode catalyst layer is the main component limiting performance. However, to some extent, GDL seem to undergo degradation as well.

These observations highlight again what is stated in the introduction: an effective mitigation of performance limitation at high current and especially when going to low Pt loadings requires a fundamental understating of transport processes in the cathode catalyst layer which is the key component in terms of performance limitation.

Freeze cycling ex-situ AST. One of the requirements for FCEVs is robustness upon freeze-thaw (F/T) cycling that regularly occurs during a life of a FCEV. Thereby cold start capability at -30°C is required [20].

In the presented study F/T cycling was carried out using MEAs from EWII Fuel Cells composed of a PFSA membranes and Pt/C catalyst at anode (0.1 $mg_{Pt}cm^{-2}$) and cathode (0.25 $mg_{Pt}cm^{-2}$). To evaluate the influence of F/T cycling on PEMFC performance decay, the cell was first characterized at BoT, then shut down and subsequently dried with N_2 before cycling 80 times between -10°C and +20°C [21]. For comparison an analogues test but without drying by N_2 was carried out. The experiment shows (Figure 8) that the influence of drying was only minor and the relative performance losses were only 10% less than without drying. The performance losses occur already at current densities of 0.5 A cm^{-2} and increases continuously with increasing current density. At 1.5 A cm^{-2} the performance loss is approximately 30%. According to EIS the impedance increases from 27 mOhm to ~35 mOhm due to F/T cycling which is likely due to damage of the catalyst layer or GDL due to freezing of captured water [21]. No change of high frequency resistance is observed indicating that no changes of the Ohmic resistance occur.

The conclusion is that the degradation rate due to F/T cycling equals roughly 0.25%/cycle determined for the performance loss at 1.4 A cm^{-2} measured after 80 cycles. This means that the end-of-life criterion (10% performance loss) is reached already after 40 cycles. Since mechanical stress due to freezing water has clearly negative effect on mass transport properties of MEA components, a mitigation strategy to avoid icing was evaluated. Specifically, the cell was flooded by a methanol-water solution before F/T cycling. The method of using methanol as antifreeze was initially published by Cho et al. [22].

The performance loss of the MEA that has been flooded by a 40% methanol-water solution during 80 F/T cycles is provided in Figure 8 (triangles). Evidently, the performance losses up to 1.5 A cm^{-2} are fully mitigated and increase sharply only upon further increasing the current density.

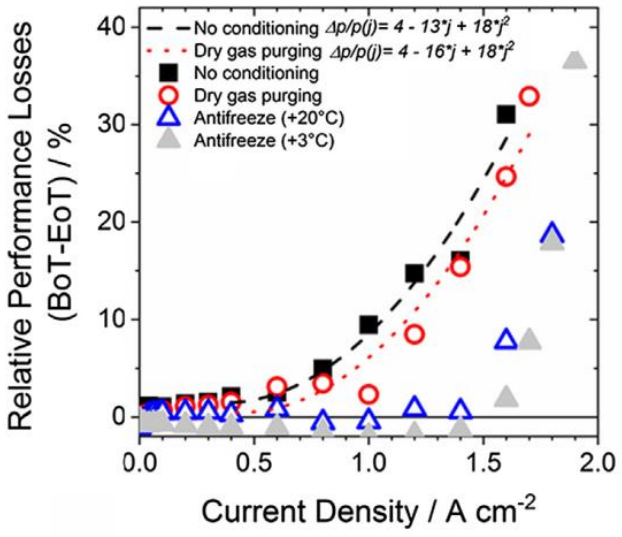

Figure 8: Relative performance losses of different F/T cycling tests. The dashed and dotted curves are parabolic fits for current densities j > 0.4 A cm^{-2} as indicated in the figure. Reprinted from Applied Energy, Vol 238, Florian Knorr, Daniel Garcia Sanchez, Johannes Schirmer, Pawel Gazdzicki, K.A. Friedrich, Methanol as antifreeze agent for cold start of automotive polymer electrolyte membrane fuel cells, Pages 1-10, Copyright 2019, with permission from Elsevier.

On-line fault diagnostics and state-of-health monitoring

Electrochemical Impedance Spectroscopy (EIS) represents an established method for on-line fault monitoring in PEMFC stacks [23, 24]. This analysis technique can provide detailed information about different processes in the stack during operation and enables the differentiation between nominal operation and operation under critical conditions, such as flooding, dry-out or reactant starvation. Thereby, we applied parallel EIS analysis on each cell of the examined stack (ZSW stationary stack with 10 cells of 96 cm^2 active area, see experimental section and Figure 1 (B)) in parallel to identify inhomogeneous operation of single cells. Commercially available 7-layer MEAs from Greenerity H500 Generation 3 were used for stack assembling. Additionally included PCBs enable the evaluation of the local current density distribution over the active area of a single cell. This allows direct observation of local gradients and temporal fluctuations of the electrochemical activity. Due to the combination of both technologies in-depth analysis of fault mechanisms could be provided and the monitoring of fuel cells could be improved in terms of response time and sensitivity towards occurring faults during fuel cell system operation.

To validate the presented methodology for monitoring of cathodic faults, the stack was operated under critical conditions for cell dry-out, for air starvation and for cathode flooding. Therefore, the relative humidity of the fed air (RH_{air}) was varied between 0% and 100% to determine the monitoring possibilities regarding cell dry out and cell flooding. Additionally, the air stoichiometry (λ_{air}) was varied between 2.0 and 1.5 to analyze air starvation issues. During these tests all parameters are controlled according to

the guidelines for reliable PEMFC stack testing defined in the European Stack Test project [10]. The results of this study at 0.5 A cm^{-2} are presented in Figure 9.

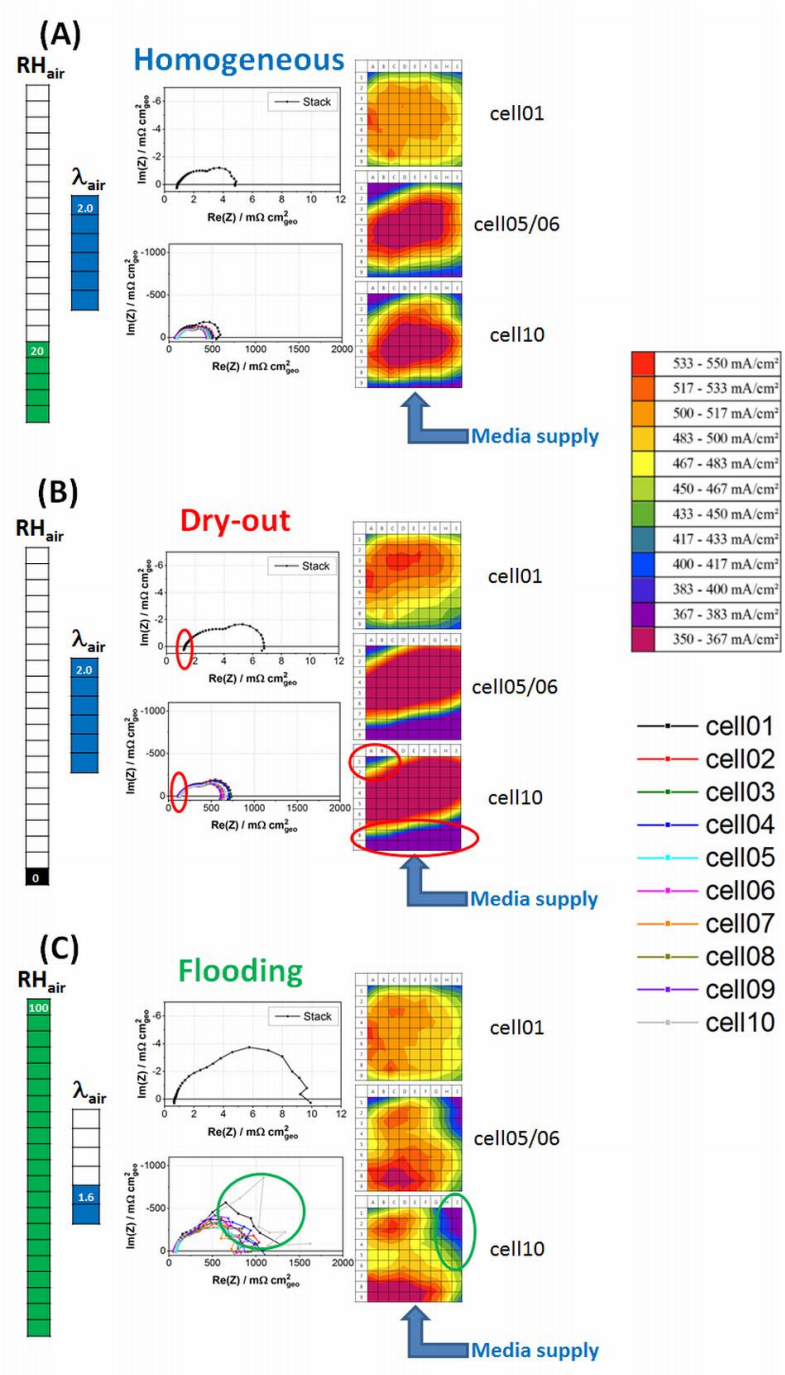

Figure 9: Monitoring of cathodic faults at 0.5 A cm² using ZSW stationary stack with 10 cells of 96 cm^2 active area. All test performed at 80 °C stack temperature, 150 kPa_{abs} gas pressure, and constant anodic conditions of 1.5 hydrogen stoichiometry and 30% relative hydrogen humidity. Panel (A) shows most homogeneous stack operation applying air stoichiometry of 2.0 and relative air humidity of 20%, (B) represents dry-out conditions without external air humidification and air stoichiometry of 2.0, and (C) demonstrates flooding conditions under fully humidified air at a stoichiometry of 1.6.

The variation of the cathodic conditions has shown that the most homogeneous stack operation could be achieved by feeding the air at stoichiometry of 2.0 with a relative humidity of 20% (Figure 9 A). Applying these conditions resulted in well humidified membranes, indicated by low resistance in the high frequency region, and low mass transport resistance, indicated by low resistance in low frequency region of the impedance spectra. Furthermore, all single cells show similar impedance behavior. PCB measurements demonstrated that the current density is uniformly distributed over the active area of the stack and the highest performance in each cell is located in the center of the active area. If non-humidified air is fed to the stack at the same stoichiometry of 2.0, cell dry-out appeared (Figure 9 B). This behavior could be detected via EIS by increased electrolyte resistance at high frequencies and via PCB by decreased current density close to the air inlet on the bottom left corner of each single cell (marked in red) as a result of the non-humidified air entering the stack. Thereby, the PCB results indicated that the membrane drying issue was more pronounced in the cells close to the media inlets (cell10) compared to cells at the end of the stack (cell01). For high air inlet humidity and low air stoichiometry, flooding of different cells becomes detectable and most obvious for fully humidified air at a stoichiometry of 1.6 (Figure 9 C). In this case, the mass transport resistance increases significantly and the voltage response at low frequencies becomes instable caused by oscillations due to liquid water in the cathodic flow field. Hence, the PCB measurements demonstrate low current density areas close to the air outlet on the upper right corner as a consequence of the accumulation of liquid water along the cathodic flow field (marked in green). Again, it was obvious in these measurements that the inhomogeneity of the single cell operation increased for cells close to the media inlet. In general, this seems to be a result of inhomogeneous gas flow distribution and temperature differences between the single cells.

Summarized, the combination of both techniques, single cell EIS and PCB, enables clearly the identification and isolation of occurring cathodic fault mechanism. Due to this finding, the monitoring methodology could be improved to avoid stack operation under such critical conditions and to increase lifetime and efficiency of the used PEMFC stacks.

Conclusions

Understanding performance limitations and degradation effects is particularly important when going to low Pt loadings (~0.1 mg cm^{-2}) as pursued by MEA development for automotive applications. A simple reduction of Pt loading by e.g. reduction of catalyst layer thickness leads to severe performance drop when going below ~0.2 mg cm^{-2} cathode Pt loading. The same applies for irreversible degradation losses that are enhanced when reduction cathodic Pt loading below ~0.2–0.3 mg cm^{-2}.

In terms of operation conditions, it is found that dynamic operation, such as required in automotive conditions, leads to lower performance losses and a significantly more homogeneous current density distribution (less prone to degradation) compared to operation at constant current. Moreover, introduction of contaminants such as Si (from gasket) and Ni (from BPP) enhance inhomogeneity of current density distribution even further; thereby contamination by Ni is more severe than by Si because it induces irreversible degradation.

Results of in-situ AST (application of mechanical stress and excess temperature) indicate that degradation of cathode catalyst layer is the major issue; however, degradation of other components (membrane, GDL) occurs as well when introducing certain stressor. The degradation rate upon applying the different ASTs were in the range 500-600 μV/h (at 1.2 A cm^{-2}) which is at least 25x faster than voltage loss expected in normal operation conditions. For instance, the F/T cycling test shows that only 40 cycles are need to induce 10% voltage loss.

The above observations highlight that going to low Pt loadings needs a fundamental understating of transport processes in the cathode catalyst layer, which is the key component in terms of performance limitation, to be able to propose mitigation strategies at material level. For instance, our recent study using a low loaded MEA with 0.16 mg cm^{-2} cathode Pt loading clearly demonstrates that increasing porosity of the cathode catalyst layer has a significant positive effect on mass transport ability of the cell [25].

It is noted that longevity of PEMFC needs to be not only addressed on material level, but also in terms of optimization of operation conditions. In this context critical or faulty operation conditions need to be continuously monitored during operation in order to mitigate them by a control algorithm.

Acknowledgments

The project focused on AST development has received funding from the Fuel Cells and Hydrogen 2 Joint Undertaking under grant agreement No 779565 (ID-Fast). This Joint Undertaking receives support from the European Union's Horizon 2020 research and innovation programme.

The presented work regarding on-line stack monitoring was realized in the COALA project (control algorithm and controller for increasing the efficiency of hybrid PEFC systems in different applications) in the framework of the Polish-German Sustainability Research Call (STAIR II). The funding for this research was received from the National Center for Research and Development (NCBR, Poland) and the Federal Ministry of Education and Research (BMBF, Germany) with the Grant No.: STAIR/6/2016 and 01LX1601, respectively.

References

1. https://www.fch.europa.eu/page/multi-annual-work-plan
2. https://www.energy.gov/eere/fuelcells/doe-technical-targets-fuel-cell-systems-and-stacks-transportation-applications
3. P. Gazdzicki, J. Mitzel, D. Garcia Sanchez, M. Schulze, and K. A. Friedrich, *J. Power Sources*, **327**, 86 (2016).
4. IPA Fact Sheet, AUTOCATALYSTS AND PLATINUM GROUP METALS (PGMs), https://ipa-news.com/index/platinum-group-metals/pgm-fact-sheets.html

5. European Automobile Manufacturers Association, http://www.acea.be/statistics/tag/category/cubic-capacity-average-power
6. A. Kongkanand and M. F. Mathias, *J. Phys. Chem. Lett.* **7**, 1127 (2016).
7. H. A. Gasteiger, J. E. Panels, and S. G. Yan, *J. Power Sources* **127**, 162 (2004).
8. P. Gazdzicki, J. Mitzel, A.M. Dreizler, M. Schulze, K. A. Friedrich, *Fuel Cells*, **18,** 270 (2018).
9. Georgios Tsotridis, Alberto Pilenga, Giancarlo De Marco, Thomas Malkow; EU Harmonised Test Protocols for PEMFC MEA Testing in Single Cell Configuration for Automotive Applications, JRC Science for Policy report, 2015, EUR 27632 EN; DOI: 10.2790/54653
10. J. Mitzel, E. Gülzow, A. Kabza, J. Hunger, S. S. Araya, P. Piela, I. Alecha, G.Tsotridis, *Int. J. Hydrogen Energy*, **41**, 21415 (2016).
11. Stack-Test Project (FCH JU Grant No. 303445), Test modules available at http://stacktest.zsw-bw.de/media-centre/test-modules
12. S. Arisetty, X. Wang, R. K. Ahluwalia, R. Mukundan, R. Borup, J. Davey, D. Langlois, F. Gambini, O. Polevaya, and S. Blanchet, *J. Electrochem. Soc.*, **159**, B455 (2012).
13. M. Schulze, E. Gülzow, S. Schönbauer, T. Knöri, and R. Reissner, *J. Power Sources*, **173**, 19 (2007)
14. M. Schulze, N. Wagner, T. Kaz, and K. A. Friedrich, *Electrochim. Acta*, **52**, 2328 (2007)
15. W. Schmittinger, A. Vahidi, *J. Power Sources*, **180**, 1 (2008).
16. S. Helmly, R. Hiesgen, T. Morawietz, X.-Z. Yuan, H. Wang, and K. Andreas Friedrich, *J. Electrochem. Soc.*, **160,** 687 (2013).
17. L. Tang et al., *J. Am. Chem. Soc.*, **132**, 596 (2010).
18. H. Liu, J. Zhang, F. D. Coms, W. Gu, B. Litteer, and H. A. Gasteiger, *ECS Trans.* **3**, 493 (2006).
19. D. G. Sanchez, T. Ruiu, I. Biswas, M. Schulze, S. Helmly, K. A. Friedrich, *J. Power Sources*, **352**, 42 (2017).
20. A.A. Amamou, S. Kelouwani, L. Boulon, K. Agbossou, *IEEE Access*. **4**, 4989 (2016).
21. F. Knorr, D. Garcia Sanchez, J. Schirmer, P. Gazdzicki, K. A. Friedrich, *Appl. Energy*, **238**, 1 (2019).
22. Cho E, Ko J-J, Ha HY, Hong S-A, Lee K-Y, Lim T-W, et al., *J. Electrochem Soc.*, 151, A661 (2004).
23. K. Darowicki, E. Janicka, M. Mielniczek, A. Zielinski, L. Gawel, J. Mitzel, J. Hunger, *Electrochimica Acta*, **292**, 383 (2018).
24. K. Darowicki, E. Janicka, M. Mielniczek, A. Zielinski, L. Gawel, J. Mitzel, J. Hunger, *Applied Energy*, **251**, 113396 (2019).
25. Talukdar, K., Delgado, S., Lagarteira, T., Gazdzicki, P., Friedrich, K.A., *J. Power Sources*, **427**, 309 (2019).